Electrical Spiking in *Escherichia coli* Probed with a Fluorescent Voltage-Indicating Protein

Joel M. Kralj, *et al.*

Science **333**, 345 (2011);
DOI: 10.1126/science.1204763

To investigate whether a common mechanism controls the change in airway shape in primary and later branch generations during normal lung growth, we examined L.L2, a left lateral secondary branch (*31*) (fig. S11, A to C). As in the control primary branches, spindle orientation in wild-type L.L2 was strongly biased toward low angles (fig. S11D). Notably, as for the primary branch, the fold-change ρ for L.L2 between t_i (55 som) and t_f (60 som) predicted on the basis of the observed spindle angle distribution closely matched the measured value (fig. S11E).

Our analysis suggests that cell division in airway epithelium may by default be oriented longitudinally and ERK1/2 activity functions as a switch to override the default orientation, with the level of ERK1/2 activity determining the probability that override will occur. Presumably, ERK1/2 activity does not itself provide any orientation cue but instead determines whether or not a cell responds to such cues. The planar cell polarity (PCP) pathway, which plays an important role in regulating mitotic spindle angle distribution in other tissues (*14*, *32*–*34*), may provide these cues. However, as yet, there is no evidence that PCP pathway genes function to regulate airway shape or spindle orientation in the lung. Indeed, these parameters were normal in lungs from *Vangl2*^{Lp} homozygotes (fig. S12).

The mechanism by which ERK1/2 signaling influences spindle orientation remains to be determined. Possibilities include effects on the centrosomal components of the mitotic spindle, on the cytoskeletal elements that control centrosome position and spindle orientation, or on some aspect of cell behavior. Consistent with observations that cell movement in presomitic mesoderm and limb bud is affected by ERK1/2 signaling (*35*, *36*), it is conceivable that high levels of signaling cause mitotic cells to rotate within the epithelium such that spindle angle with respect to the airway longitudinal axis is altered.

The hypothesis that RAS-regulated ERK1/2 signaling influences airway shape change by regulating mitotic spindle angle distribution not only explains the adverse effects on airway shape of increasing ERK1/2 activity, but also posits a role for ERK1/2 signaling in controlling normal airway shape change during development. It is tempting to speculate that such a mechanism also regulates epithelial tube shape changes in other branched organs. Moreover, our data identify sprouty genes as key regulators that function to ensure that the shape changes required for normal development occur.

References and Notes

1. E. R. Weibel, D. M. Gomez, *Science* **137**, 577 (1962).
2. Information on materials and methods is available on *Science* Online.
3. J. S. Huxley, G. Teissier, *Nature* **137**, 780 (1936).
4. E. E. Morrisey, B. L. Hogan, *Dev. Cell* **18**, 8 (2010).
5. B. D. Harfe *et al.*, *Cell* **118**, 517 (2004).
6. E. L. Jackson *et al.*, *Genes Dev.* **15**, 3243 (2001).
7. A. Young *et al.*, *Adv. Cancer Res.* **102**, 1 (2009).
8. Y. Liu *et al.*, *Curr. Biol.* **14**, 897 (2004).
9. D. Dankort *et al.*, *Genes Dev.* **21**, 379 (2007).
10. S. Courtois-Cox *et al.*, *Cancer Cell* **10**, 459 (2006).
11. J. F. Ohren *et al.*, *Nat. Struct. Mol. Biol.* **11**, 1192 (2004).
12. J. S. Sebolt-Leopold, R. Herrera, *Nat. Rev. Cancer* **4**, 937 (2004).
13. A. T. Shaw *et al.*, *Genes Dev.* **21**, 694 (2007).
14. S. Saburi *et al.*, *Nat. Genet.* **40**, 1010 (2008).
15. E. Fischer *et al.*, *Nat. Genet.* **38**, 21 (2006).
16. E. K. Kieserman, J. B. Wallingford, *J. Cell Sci.* **122**, 2481 (2009).
17. N. Hacohen, S. Kramer, D. Sutherland, Y. Hiromi, M. A. Krasnow, *Cell* **92**, 253 (1998).
18. G. Minowada *et al.*, *Development* **126**, 4465 (1999).
19. M. Fürthauer, F. Reifers, M. Brand, B. Thisse, C. Thisse, *Development* **128**, 2175 (2001).
20. J. M. Mason, D. J. Morrison, M. A. Basson, J. D. Licht, *Trends Cell Biol.* **16**, 45 (2006).
21. K. Sekine *et al.*, *Nat. Genet.* **21**, 138 (1999).
22. H. Min *et al.*, *Genes Dev.* **12**, 3156 (1998).
23. L. De Moerlooze *et al.*, *Development* **127**, 483 (2000).
24. S. Bellusci, J. Grindley, H. Emoto, N. Itoh, B. L. Hogan, *Development* **124**, 4867 (1997).
25. W. V. Cardoso, J. Lü, *Development* **133**, 1611 (2006).
26. K. Shim, G. Minowada, D. E. Coling, G. R. Martin, *Dev. Cell* **8**, 553 (2005).
27. O. D. Klein *et al.*, *Dev. Cell* **11**, 181 (2006).
28. O. D. Klein *et al.*, *Development* **135**, 377 (2008).
29. M. A. Basson *et al.*, *Dev. Cell* **8**, 229 (2005).
30. J. S. Colvin, A. C. White, S. J. Pratt, D. M. Ornitz, *Development* **128**, 2095 (2001).
31. R. J. Metzger, O. D. Klein, G. R. Martin, M. A. Krasnow, *Nature* **453**, 745 (2008).
32. L. A. Baena-López, A. Baonza, A. García-Bellido, *Curr. Biol.* **15**, 1640 (2005).
33. Y. Gong, C. Mo, S. E. Fraser, *Nature* **430**, 689 (2004).
34. B. Ciruna, A. Jenny, D. Lee, M. Mlodzik, A. F. Schier, *Nature* **439**, 220 (2006).
35. B. Bénazéraf *et al.*, *Nature* **466**, 248 (2010).
36. J. Gros *et al.*, *Curr. Biol.* **20**, 1993 (2010).

Acknowledgments: We are grateful to J. Licht and J. Zallen for insightful and helpful suggestions; B. Hann for technical advice; K. Thorn (Nikon Imaging Center at UCSF/QB3) for imaging assistance; and D. Hom, P. Ghatpande, C. Firkus, and E. Yu for technical assistance. We also thank members of the Martin, Metzger, and Marshall laboratories and M. Barna, P. Devine, U. Grieshammer, J. Jeong, O. Klein, M. Kumar, S. Luschnig, A. Mogilner, S. Rafelski, and S. Greenberg for helpful comments on the manuscript. This work was supported by NIH grants R01 CA131201 (to M.McM.), R01 GM077004 (to W.F.M), and R01 CA78711 and R01 DE17744 (to G.R.M.). W.F.M. was supported by the W. M. Keck Foundation; R.J.M. was supported by the UCSF Program for Breakthrough Biomedical Research, which is funded in part by the Sandler Foundation; N.T. was supported by an American Heart Association postdoctoral fellowship and NIH training grant 5T32HL007185.

Supporting Online Material

www.sciencemag.org/cgi/content/full/333/6040/342/DC1
Materials and Methods
SOM Text
Figs. S1 to S12
References

25 February 2011; accepted 16 May 2011
10.1126/science.1204831

Electrical Spiking in *Escherichia coli* Probed with a Fluorescent Voltage-Indicating Protein

Joel M. Kralj,[1] Daniel R. Hochbaum,[2] Adam D. Douglass,[3] Adam E. Cohen[1,4]*

Bacteria have many voltage- and ligand-gated ion channels, and population-level measurements indicate that membrane potential is important for bacterial survival. However, it has not been possible to probe voltage dynamics in an intact bacterium. Here we developed a method to reveal electrical spiking in *Escherichia coli*. To probe bacterial membrane potential, we engineered a voltage-sensitive fluorescent protein based on green-absorbing proteorhodopsin. Expression of the proteorhodopsin optical proton sensor (PROPS) in *E. coli* revealed electrical spiking at up to 1 hertz. Spiking was sensitive to chemical and physical perturbations and coincided with rapid efflux of a small-molecule fluorophore, suggesting that bacterial efflux machinery may be electrically regulated.

Bacterial membrane potential provides a major component of the driving force for oxidative phosphorylation, membrane transport, and flagellar motion. Yet this voltage is inaccessible to techniques of conventional electrophysiology, owing to the small size of bacteria and the presence of a cell wall. Little is known about the electrophysiology of bacteria at the level of single cells (*1*).

We developed a genetically encoded optical indicator of membrane potential, V_m, in bacteria. The starting protein was green-absorbing proteorhodopsin (GPR), a light-driven proton pump found in bacteria in the ocean (*2*–*4*). In the wild, light-driven transport of a proton through GPR changes the color of the protein. We sought to run GPR backward: to use V_m to reposition a proton, and thereby to induce a color shift (*5*).

The dominant color-determining moiety in GPR is the Schiff base (SB), which links the

[1]Department of Chemistry and Chemical Biology, Harvard University, Cambridge, MA 02138, USA. [2]Applied Physics Program, School of Engineering and Applied Sciences, Harvard University, Cambridge, MA 02138, USA. [3]Department of Molecular and Cellular Biology, Harvard University, Cambridge, MA 02138, USA. [4]Department of Physics, Harvard University, Cambridge, MA 02138, USA.

*To whom correspondence should be addressed. E-mail: cohen@chemistry.harvard.edu

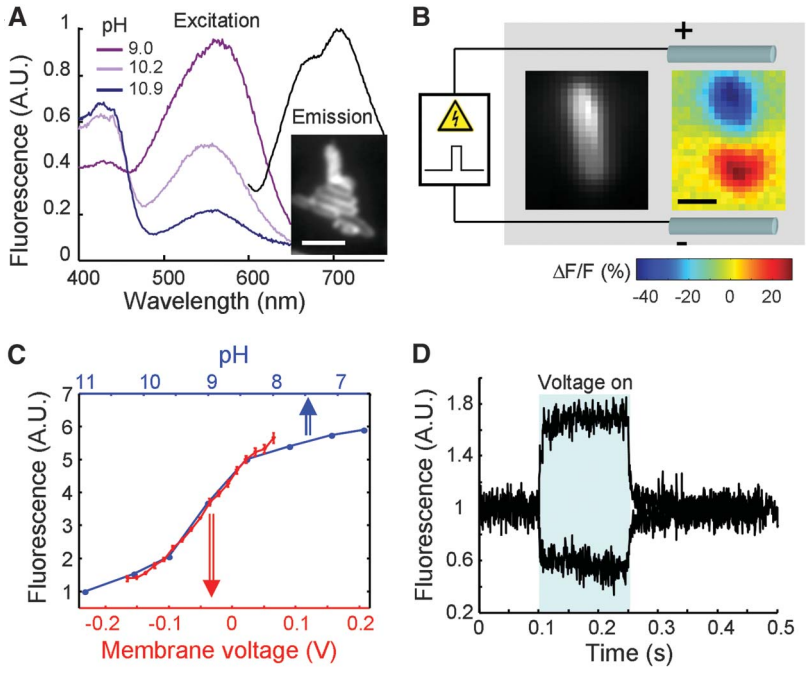

Fig. 1. PROPS is a fluorescent indicator of bacterial membrane potential. (**A**) Fluorescence spectra of purified PROPS as a function of pH, indicating titration of the Schiff base, with a pK_a of 9.6 (versus >12 in wild-type GPR). Peak emission at λ = 710 nm, quantum yield 1.0 × 10^{-3}. PROPS yielded 9.1 times as many photons per molecule before photobleaching as did the GFP (green fluorescent protein) homolog Venus (*6*). (Inset) Image of *E. coli* visualized via fluorescence of PROPS (scale bar, 5 μm). Cells were only fluorescent in the presence of retinal (fig. S11). Expression at ~28,000 copies per cell had a minor effect on growth rate in rich medium (*6*). Membrane fractionation yielded protein associated only with the inner membrane (*6*). (**B**) Spatially resolved change in fluorescence in a single cell subject to ITV. Scale bar, 2 μm. Electrodes not shown to scale; actual spacing, 1.6 mm. (**C**) Comparison of pH- and voltage-dependent fluorescence of PROPS. A change in membrane potential of 102 mV was equivalent to a change in pH of 1 unit in its effect on fluorescence. The sensitivity was $\Delta F/F$ = 150% per 100 mV (*6*). Error bars represent SEM. (**D**) Time course of the fluorescence response to positive and negative steps in membrane potential. Data in (B) to (D) represent the average of 20 voltage pulses.

retinal to the protein core. When the SB was protonated, the protein was pink and weakly fluorescent in the near infrared; when the SB was deprotonated, the protein was yellow and nonfluorescent (fig. S1). We hypothesized that a change in V_m could alter the local electrochemical potential of protons on the SB, and thereby tip the acid-base equilibrium between the fluorescent and nonfluorescent states (fig. S2) (*6*). However, the pK_a (acid dissociation constant) of the SB was >12, indicating that protons were bound too tightly to be removed by physiological V_m. The mutant GPR^{D97N} had a SB pK_a of 9.6, showed pH-dependent fluorescence (Fig. 1A), and also lacked light-induced proton pumping (*7*), making it a promising candidate voltage sensor. We call GPR^{D97N} a proteorhodopsin optical proton sensor (PROPS).

Induced transmembrane voltage (ITV) (*8*) was used to calibrate fluorescence versus V_m in intact *Escherichia coli* expressing PROPS (*6*). Voltage pulses were applied to field-stimulation electrodes spanning a plate of cells. During the voltage pulse, the depolarized end of each cell became transiently bright, and the hyperpolarized end became transiently dark (Fig. 1B), indicating a cytoplasm-exposed SB (*6*). The fluorescence of PROPS was five times as bright at an induced V_m of +70 mV than at −170 mV (Fig. 1C). The response to a voltage step occurred with a time constant of 4.7 ms (Fig. 1D).

E. coli expressing PROPS were imaged at the interface of a coverslip and an agarose pad containing minimal medium. Unexpectedly, many cells exhibited quasi-periodic cell-wide blinks in fluorescence (Fig. 2 and movies S1 and S2). The blinks occurred simultaneously over an entire cell,

Fig. 2. *E. coli* expressing PROPS show transient flashes of fluorescence. (**A**) Dynamics of fluorescence intensity (I = 4 W/cm^2) of five single cells in a freshly grown sample under an agarose pad containing minimal medium at pH 7.0. (**B**) Top: Simultaneous recording of PROPS and pHluorin fluorescence in *E. coli* treated with CCCP (50 μg/ml) during steps in pH_o. Bottom: Intensities of PROPS and pHluorin in a single cell during a blink, in the absence of CCCP. (**C**) Simultaneous measurement of fluorescence (top) and rotation (bottom) of a cell (strain JY29 Δ*cheY*) tethered by its flagellum to a coverslip. Construction of the rotary kymograph is described in (*6*).

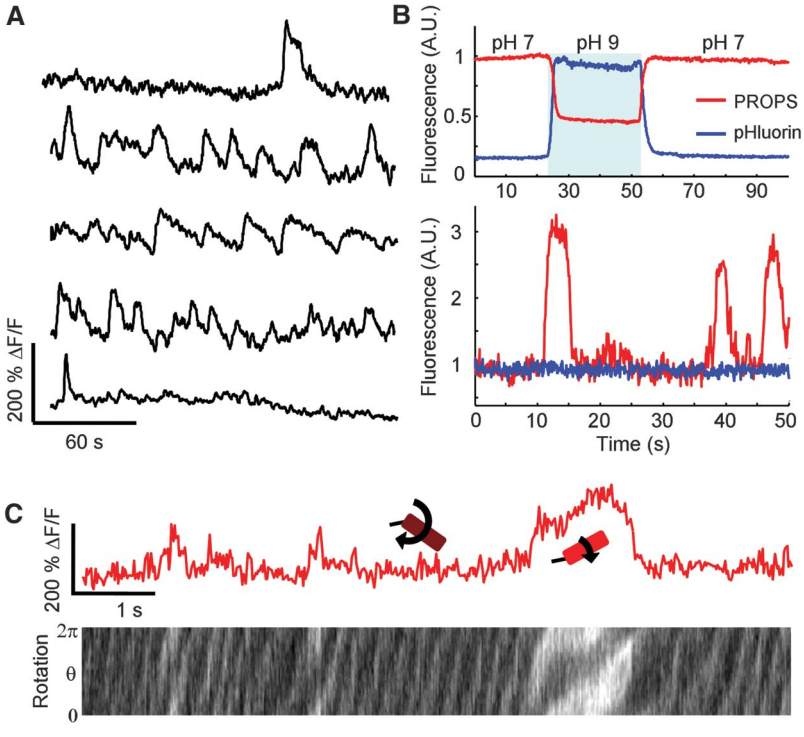

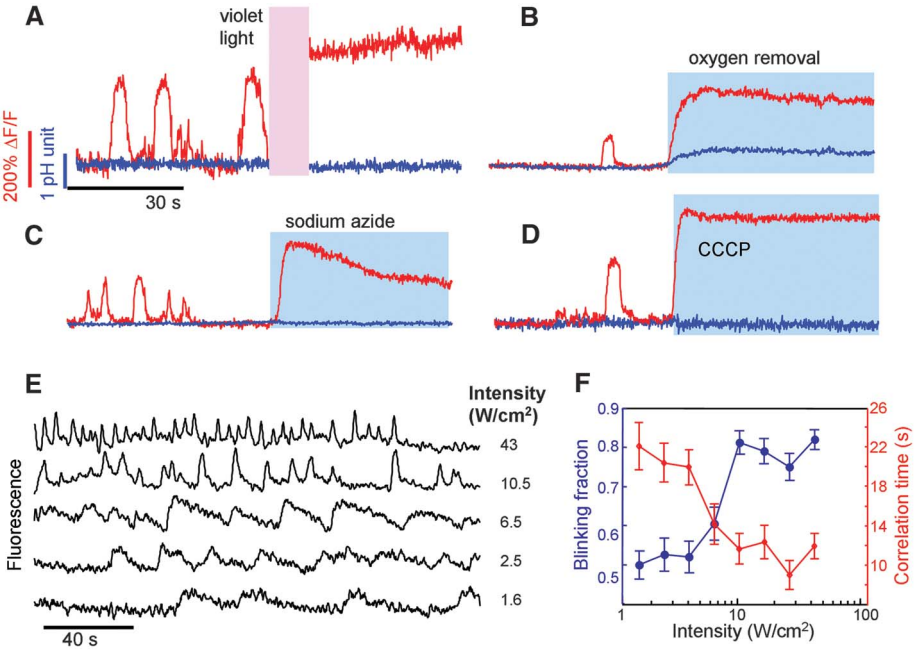

Fig. 3. Single-cell responses to metabolic perturbations. Fluorescence of pHluorin and PROPS were recorded simultaneously to indicate responses of pH_i and V_m, respectively. (**A**) Violet light (100 W/cm^2). Leakage of the violet light into the pHluorin and PROPS channels prevented acquisition of data during the perturbation. (**B**) Removal of oxygen. (**C**) Sodium azide (10 mM). (**D**) CCCP (50 μg/ml). Scale bars in (A) apply to data in (A) to (D). Colored bars indicate duration of the perturbation. (**E**) Blinking of *E. coli* expressing PROPS as a function of illumination intensity. (**F**) Blinks became more prevalent (blue) and shorter (red) at higher illumination intensity. Error bars represent SEM. Between 114 and 211 cells were analyzed at each intensity.

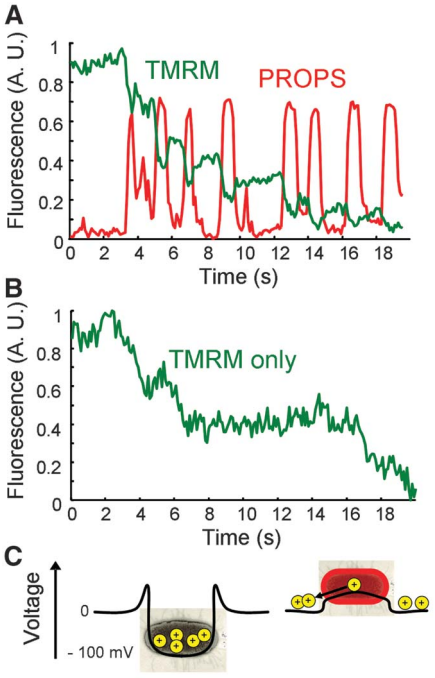

Fig. 4. Blinks are accompanied by efflux of a cationic dye. (**A**) Simultaneous measurement of fluorescence from PROPS and TMRM. Blinks in PROPS (red) coincided with sudden drops in concentration of TMRM (green). (**B**) Cells not expressing PROPS showed stepwise efflux of TMRM, suggesting that electrical spiking occurred in the absence of PROPS. (**C**) Model for voltage-regulated cationic efflux. The resting potential of −80 to −120 mV is necessary for metabolism, but opposes cationic efflux. Transient depolarization lowers the barrier to efflux.

to within the 10-ms time resolution of our imaging system. Blinks were uncorrelated between neighboring cells.

We observed a variety of blinking behaviors within a nominally homogeneous population of cells (Fig. 2A). Some cells were dark for many minutes, blinked once, and then returned to darkness; others had periods of quiescence punctuated by bursts of blinking. Blinks had durations from 1 to 40 s with rapid rise times followed by slower decays. The intensity of blinks varied within and between cells, but occasionally we observed periodic bursts of blinking to the same brightness. Some cells remained bright for many minutes, and some remained dark. Many individual cells exhibited different motifs at different times. Blinking cells continued to grow and divide when incubated in the dark at 35°C (fig. S3).

To determine whether blinks arose from fluctuations in internal pH (pH_i), we coexpressed the cytoplasmic pH indicator super-ecliptic pHluorin (*9*) and PROPS, and simultaneously observed the fluorescence of both (Fig. 2B). The pHluorin indicated intracellular pH at the single-cell level with a response time of <1 s and a precision of better than 0.1 pH units (*6*). During a blink, pH_i remained constant to within measurement precision (Fig. 2B and fig. S4). Thus, blinks did not arise from fluctuations in pH_i.

To determine whether the blinks arose from electrical fluctuations, we used the torque of the flagellar motor as an indicator of the protonmotive force (PMF) (*10*). Cells of strain JY29 were adhered to a coverslip by a single flagellum, and we monitored the blinking of PROPS and the rate of rotation of the cell body simultaneously (*6*). During a blink, the rotation slowed or stopped, indicating that blinks coincided with a loss of PMF (Fig. 2C, fig. S5, and movie S3). The loss of PMF, but stable pH_i, during a blink implied that blinks arose from electrical depolarization.

Lipophilic voltage-sensitive dyes (VSDs) did not label blinking cells (*6*) and thus were unable to provide independent confirmation that blinks were electrical. Within a field of view containing blinking and nonblinking cells, the VSDs only labeled nonblinking cells (fig. S6). The reason for this heterogeneous labeling is unclear. Previous efforts to use VSDs in *E. coli* were unsuccessful (*11*).

We examined the effect of metabolic state on blinking and pH_i in cells coexpressing PROPS and super-ecliptic pHluorin. Interruption of aerobic respiration caused blinking to cease and all cells to become bright in the PROPS channel. This behavior was seen for inhibition of the electron-transport chain by exposure to intense violet light (Fig. 3A) (*12*) or by removal of oxygen (Fig. 3B). Inhibition of the F_1–adenosine triphosphatase (ATPase) by sodium azide (10 mM, Fig. 3C) (*13*) and dissipation of the PMF by carbonyl cyanide *m*-chlorophenyl hydrazone (CCCP; 50 μg/ml, Fig. 3D) (*14*) induced similar responses (movies S4 to S7). None of these treatments affected the fluorescence of purified PROPS. Thus, *E. coli* needed to be alive and undergoing aerobic respiration to blink.

When the experiments above were performed at $pH_i \approx pH_o$ (external pH; corresponding to pH_o = 8.3, fig. S7), the perturbations induced minimal change in pH_i (Fig. 3). At other values of pH_o, the perturbations caused gradual equilibration of pH_i with pH_o, indicating a failure of pH homeostasis (fig. S8).

The intensity of the red laser used to image PROPS affected the shape and frequency of the blinks. At higher illumination intensity the blinks were briefer and more intense, and came in more regular and higher-frequency pulse trains (Fig. 3, E and F). The mechanism by which illumination enhanced blinking is not known; but we note that *E. coli* contain endogenous chromophores in their electron transport chain with absorption throughout the visible spectrum (*15*). Heating by the imaging laser is expected to be negligible (*6*).

The enhancement of blinking by increased laser power suggested that blinking might form part of the stress response mechanism in *E. coli*. We thus tested whether blinking was associated with cationic efflux, another important mechanism of stress response.

We observed surprising dynamics of a cationic membrane-permeable dye, tetramethyl rhodamine methyl-ester (TMRM), in blinking *E. coli*. As expected for this Nernstian voltage indicator (*16*), TMRM gradually accumulated in the cytoplasm over ~10 min. However, blinks in PROPS fluorescence coincided with precipitous stepwise drops in TMRM fluorescence that showed little or no recovery after the blink (Fig. 4A). The duration of the step in TMRM fluorescence coincided with the duration of the blink: At moderate intensities of red illumination (I = 10 W/cm^2) steps lasted less than 200 ms, whereas under little or no red illumination steps typically lasted several seconds (fig. S9). Stepwise disappearance of TMRM was also observed in cells without the PROPS plasmid, when only dim green illumination was used to image the TMRM (30 mW/cm^2; Fig. 4B and fig. S10). The duration of these steps was comparable to that of steps in cells with PROPS under dim red illumination (2 W/cm^2). The rapid disappearance of TMRM during a blink suggested an active-transport mechanism. Dissipation of V_m lowers the thermodynamic barrier to cationic efflux (Fig. 4C) (*6*). A concurrent dissipation of V_m and increase in membrane permeability would be sufficient to induce cationic efflux. PMF-dependent efflux of other cationic dyes has been observed in *E. coli* (*17*) in population-level assays that are insensitive to the dynamics of individual cells.

Bacterial electrophysiology is likely to differ in several key regards from its eukaryotic version due to the comparatively small surface area, yet high surface-to-volume ratio found in bacteria. With a typical membrane capacitance between 10^{-14} and 10^{-13} F, a single ion channel with a conductivity of 100 pS can alter the membrane potential with a time constant of 10^{-3} to 10^{-4} s. In contrast, neurons only fire through the concerted action of a large number of ion channels. Thus, bacterial electrophysiology is likely to be dominated by stochastic opening of individual ion channels and pores. Additionally, the ionic composition of bacteria is less robust than that of eukaryotes. A bacterium with a volume of 1 fl and a cytoplasmic Na^+ concentration of 10 mM contains only ~10^7 ions of Na^+. A single ion channel passing a current of 2 pA can deplete this store in less than 1 s. These simple estimates show that some of the tenets of neuronal electrophysiology may need rethinking in the context of bacteria.

References and Notes

1. B. Martinac, Y. Saimi, C. Kung, *Physiol. Rev.* **88**, 1449 (2008).
2. O. Béjà, E. N. Spudich, J. L. Spudich, M. Leclerc, E. F. DeLong, *Nature* **411**, 786 (2001).
3. O. Béjà *et al.*, *Science* **289**, 1902 (2000).
4. J. L. Spudich, C. S. Yang, K. H. Jung, E. N. Spudich, *Annu. Rev. Cell Dev. Biol.* **16**, 365 (2000).
5. P. Kolodner, E. P. Lukashev, Y. C. Ching, D. L. Rousseau, *Proc. Natl. Acad. Sci. U.S.A.* **93**, 11618 (1996).
6. Materials and methods are available as supporting material on *Science* Online.
7. A. K. Dioumaev, J. M. Wang, Z. Bálint, G. Váró, J. K. Lanyi, *Biochemistry* **42**, 6582 (2003).
8. G. Pucihar, T. Kotnik, D. Miklavčič, *J. Vis. Exp.* **33**, 1659 (2009).
9. G. Miesenböck, D. A. De Angelis, J. E. Rothman, *Nature* **394**, 192 (1998).
10. D. C. Fung, H. C. Berg, *Nature* **375**, 809 (1995).
11. D. Novo, N. G. Perlmutter, R. H. Hunt, H. M. Shapiro, *Cytometry* **35**, 55 (1999).
12. G. D. Sprott, W. G. Martin, H. Schneider, *Photochem. Photobiol.* **24**, 21 (1976).
13. T. Noumi, M. Maeda, M. Futai, *FEBS Lett.* **213**, 381 (1987).
14. A. K. Joshi, S. Ahmed, G. Ferro-Luzzi Ames, *J. Biol. Chem.* **264**, 2126 (1989).
15. W. J. Ingledew, R. K. Poole, *Microbiol. Rev.* **48**, 222 (1984).
16. C. J. Lo, M. C. Leake, T. Pilizota, R. M. Berry, *Biophys. J.* **93**, 294 (2007).
17. J. A. Bohnert, B. Karamian, H. Nikaido, *Antimicrob. Agents Chemother.* **54**, 3770 (2010).

Acknowledgments: We thank K. Rothschild for helpful discussions and for the GPR plasmid. We also thank H. Berg, R. Losick, J. Yuan, H. Inada, A. Garner, and D. Kahne for helpful discussions. G. Miesenbock provided the pHluorin plasmid. A. Fields, H. Bayraktar, V. Venkatachalam, and L. Bane helped with measurements. This work was supported by the Harvard Center for Brain Science, an Intelligence Community Postdoctoral Fellowship (J.M.K.), a National Science Foundation Graduate Fellowship (D.R.H.), a Helen Hay Whitney Postdoctoral Fellowship (A.D.D.), and a Charles A. King Trust Postdoctoral Fellowship (A.D.D). J.M.K., A.D.D., and A.E.C. have applied for a patent on PROPS as a sensor of membrane potential.

Supporting Online Material

www.sciencemag.org/cgi/content/full/333/6040/345/DC1
Materials and Methods
SOM Text
Figs. S1 to S11
Tables S1 to S6
References (*18*–*33*)
Movies S1 to S7

24 February 2011; accepted 31 May 2011
10.1126/science.1204763

Precise Manipulation of Chromosomes in Vivo Enables Genome-Wide Codon Replacement

Farren J. Isaacs,[1]*†‡ Peter A. Carr,[2,3]*‡§ Harris H. Wang,[1,4,5,6]* Marc J. Lajoie,[1,7] Bram Sterling,[2,3] Laurens Kraal,[1] Andrew C. Tolonen,[1] Tara A. Gianoulis,[1,6] Daniel B. Goodman,[1,5] Nikos B. Reppas,[8] Christopher J. Emig,[9] Duhee Bang,[10] Samuel J. Hwang,[11] Michael C. Jewett,[1,12] Joseph M. Jacobson,[2,3] George M. Church[1,6]

We present genome engineering technologies that are capable of fundamentally reengineering genomes from the nucleotide to the megabase scale. We used multiplex automated genome engineering (MAGE) to site-specifically replace all 314 TAG stop codons with synonymous TAA codons in parallel across 32 *Escherichia coli* strains. This approach allowed us to measure individual recombination frequencies, confirm viability for each modification, and identify associated phenotypes. We developed hierarchical conjugative assembly genome engineering (CAGE) to merge these sets of codon modifications into genomes with 80 precise changes, which demonstrate that these synonymous codon substitutions can be combined into higher-order strains without synthetic lethal effects. Our methods treat the chromosome as both an editable and an evolvable template, permitting the exploration of vast genetic landscapes.

The conservation of the genetic code, with minor exceptions (*1*), enables exchange of gene function among species, with viruses, and across ecosystems. Experiments involving fundamental changes to the genetic code could substantially enhance our understanding of the origins of the canonical code and could reveal new subtleties of how genetic information is encoded and exchanged (*1*, *2*). Modifying the canonical genetic code could also lead to orthogonal biological systems with new properties. For instance, a new genetic code could prevent the correct translation of exogenous genetic material and lead to the creation of virus-resistant organisms. Additionally, a recoded genome could enhance the incorporation of unnatural amino acids into proteins, because existing suppressor systems must compete with native translation factors (*3*–*5*).

The construction of a new genetic code requires methods to manipulate living organisms at a whole-genome scale. Such methods are only now becoming attainable through the advent of advanced tools for synthesizing, manipulating, and recombining DNA (*6*). This has led to a number of impressive genome-scale studies, which include removing transposable elements (*7*), refactoring phage genomes (*8*), genome merging (*9*), whole-genome synthesis (*10*), and transplantation (*11*). Whole-genome de novo synthesis offers the ability to create new genomes without a physical template. Its main limitations are the cost of accurate in vitro DNA assembly and introduction of synthetic DNA into organisms (*12*). For